# STUDY OF THE FIRST ACCELEROGRAMS RECORDED IN ECUADOR DURING THE $M_W$ = 7.8 PEDERNALES 2016 EARTHQUAKE

O. Lara(1) D. Toro(2) O. Lopez3

(1)*Director IAEE. President SISMICA Consulting Engineers, ottonlara@hotmail.com*
(2)*Structural Engineer SISMICA Consulting Engineers, danieltorocastillo@yahoo.com*
(3)*Professor Universidad Central de Venezuela, oalsf@yahoo.com*

***Abstract*** The accelerograms of the Mw = 7.8 Pedernales, Ecuador 2016 earthquake were the first ever recorded in Ecuador by the National Network of the Instituto de Geofísica de la Escuela Politécnica Nacional (IGEPN). The subduction earthquake, induced by the slip of the Oceanic plate under the South American plate, was captured by 22 accelerographic stations in the Country, 3 of them on soft soil locations. The objective of this research is to study the characteristics of the soft soil records in the 3 stations, two of them in the most populated city of the Country: Guayaquil, 3 million inhabitants, located 300Km south of the epicenter but, 170Km from the rupture area, and the other in the small city of Chone, 34Km to the rupture area, and 116Km south east from the epicenter. The study contains analysis of the records: frequency contents, durations, elastic and inelastic acceleration spectra, input relative energy spectra and PGA relations among the records studied. The characteristics mentioned are compared to records from subduction earthquakes recorded on soft soils in other parts of the world and to records from crustal earthquakes.

*Keywords: Ecuador, Mexico earthquakes; soft soils; record characteristics; comparisons*

## 1. Introduction

On April 16 2016, at 19:00 hours, the severe Mw 7.8 subduction Pedernales earthquake, strongly hit the central coast of Ecuador causing the dead to more than 600 persons and damage and collapses in several towns located within the rupture area, one of them Pedernales, 29Km SW of the epicenter, and cities like Chone, Portoviejo and Manta, situated between 120 and 170Km SE and SW of the epicenter, Fig.1. The effect of the earthquake was also felt in Guayaquil, the largest city of the Country at about 300Km SE of the epicenter but, 170Km from the ruptured area, Fig. 1, causing damage and collapses. The estimated cost of the earthquake was more than 2 billion dollars.

According to IGPN, 2016 [1], the depth was 21Km, and according to GEER-ATC, 2016 [2] IGEPN-LMI SVAN, 2016, [3], rupture length was 100Km and 80Km wide, giving 8000 square kilometers of a reverse fault that is the rupture area along the interface between the Oceanic and the Continental plates. The rupture was originated by the subduction of the Oceanic plate, GEER, 2016, IGEPN-LMI SVAN, 2016, Fig.1.

The earthquake was captured by 22 accelerographic stations of the IGEPN Network, and are the first records ever captured in the country. Out of the 7 recorded in the coastal area, 3 were on soft soils, type E-F, in stations: ACHN in Chone, AGY1, AGY2, in Guayaquil, 1 on soil type D: APED, in Pedernales, and 1 on rock type B: AGYE in Guayaquil. These 5 records were chosen for this study. Fig.1 shows the acceleration components of 4 of those records (APED, ACHN, AGYE, AGY2).

The focus of this research is to study, the effects of the coastal records on elastic (ERS) and inelastic (IRS) response spectra and also, the effects of structure characteristics on ERS and IRS. To compare results such as effects of distant subduction and closer crustal ground motions on soft soils, records captured on SCT station in CD-MEX during the 1985 Michoacán subduction earthquake, the 2017 Chiapas, also subduction earthquake, and the 2017 Puebla crustal earthquake, are used. Finally, TAK-000 record from Kobe 1995, and LGPC-000 record from Loma Prieta 1987, earthquakes, both crustal, are used for comparisons. In addition, a brief summary of the attenuation analysis performed by Singaucho et al. [1] is presented here.

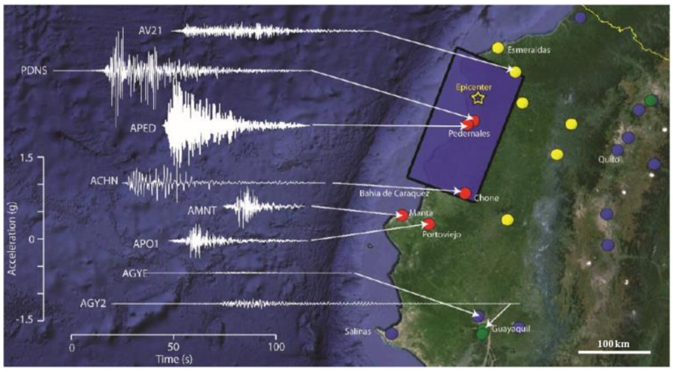


Fig. 1 Coastal area, locations of some affected cities and recorded accelerations in EW direction. (Adapted from GEER, 2016)

## 2. Analysis of the records

### 2.1 Characteristics of the records

The main characteristics of the two horizontal components of the selected records are shown in Table 1: distance from station to epicenter, $V_{s30}$, soil type, PGA, period $T_g$ computed using Fourier spectrum, $T_a$ computed from the acceleration spectrum, and $T_e$ from the relative input energy spectrum, and total, Bolt and Trifunac durations. $T_g$, $T_a$ and $T_e$ are periods corresponding to the main peak of the spectrum.

PGA attenuation ratio is defined as: PGA ratio = PGA (station) (maximum horizontal acceleration)/PGA (max recorded), where PGA (max recorded) is 1.4g captured in APED-EW record.

PGA ratios in soft soils, type E-F, Table 1, are: 24% for ACHN, 6.8% for AGY2, 4,5% for AGY1 and, 1.35 % for AGYE, rock type A, GEER, 2016. Local PGA ratio for soft soil, in Guayaquil, is: AGY1/AGY2 = 0.73 and, PGA amplification ratio between rock and soft soil is: AGY2/AGYE = 4.8. PGA ratios show important wave attenuation from Pedernales to Chone, 116Km away, and to Guayaquil, at about 300Km, Fig.1. Amplification within soft soil and between soft soil and rock, in Guayaquil, is also important.

As a comparison, PGA = 0.17g in SCT1M-N90E, (M for the 1985 Michoacan earthquake), was 1.21 times the PGA = 0.14g in CALE-S90E, rock site, located 19Km away of the Michoacan epicenter. The ratio, larger than 1.0, means a great soft soil amplification in SCT1M, 406Km away from CALE station. Within CD-MEX, PGA in SCT1(M) station was 4.25 times PGA in CUMV-S90E, located on rock in the UNAM Campus. Data for CALE and CUMV are in UNAM network.

HMTT-N00E recorded on rock in Puebla, 60 Km from the epicenter, Puebla 2017 earthquake, was 0.17g while, in SCT2P-N00E (P for Puebla) station, 120Km from the epicenter, was 0.09g therefore, PGA attenuation ratio is 0.53. The closest record to the epicenter in Chiapas earthquake was SCRU-N00E on rock, 197Km from the epicenter, and PGA was 0.3g. PGA for SCT2C-N00E (C for Chiapas) was 0.025g then, PGA ratio is 0.08. SCT2C is 744Km away from epicenter, in the Pacific Ocean, and 547 Km away from station SCRU. Data for HMTT and SCRU are in UNAM network.

PGA amplification ratios in SCT station, respect to CUPS-N90E and CUPSC-N90E records on rock in CD-MEX-UNAM, for Puebla and Chiapas earthquakes are $\frac{0.09}{0.06} = 1.25$, and $\frac{0.025}{0.009} = 2.8$, respectively.

There are variations of wave propagation in Mexican earthquakes: amplification in SCT soft soil for the subduction Michoacan earthquake, attenuation for Puebla and Chiapas, crustal and subduction earthquakes, respectively. Within CD-MEX, soft soils amplify the rock signal. In Ecuador, attenuation with distance is higher than in Mexico for Michoacan earthquake but, amplification soil/rock in Guayaquil, is similar to SCT1M/rock but, larger than SCT2P/rock (crustal) and SCT2C/rock (subduction).

Table 1 Characteristics of selected records

| EVENT | $M_w$ | RECORD | Distance Epicenter-Station, Km | $V_{s30}$ (m/s) | Soil Type | PGA (g) | $T_g$ (s) | $T_a$ (s) | $T_e$ (s) | Total Duration $t_{d\ total}$ (s) | Bolt significant duration $t_{d\ Bolt}$ (s) | Trifunac significant duration $t_{d\ Trif}$(s) |
|---|---|---|---|---|---|---|---|---|---|---|---|---|
| **PEDERNALES EARTHQUAKE** | | | | | | | | | | | | |
| **PEDERNALES EARTHQUAKE, 2016-04-16 *** | **7.8** | APED EW | 36 | 228 | D | 1.40 | 0.60 | 0.16 | 0.65 | 72 | 58 | 28 |
| | | APED NS | 36 | 228 | D | 0.83 | 0.48 | 0.50 | 0.50 | 72 | 57 | 30 |
| | | ACHN EW | 120 | 157 | E | 0.33 | 1.33 | 1.30 | 1.35 | 100 | 40 | 30 |
| | | ACHN NS | 120 | 157 | E | 0.37 | 1.45 | 1.45 | 1.45 | 100 | 30 | 25 |
| | | AGY1 EW | 292 | 178 | E | 0.06 | 1.65 | 1.70 | 1.70 | 217 | 4 | 59 |
| | | AGY1 NS | 292 | 178 | E | 0.07 | 0.80 | 0.80 | 1.65 | 217 | 3 | 63 |
| | | AGY2 EW | 286 | 101 | E | 0.09 | 1.70 | 1.70 | 1.70 | 202 | 19 | 67 |
| | | AGY2 NS | 286 | 101 | E | 0.10 | 1.70 | 0.45 | 1.70 | 202 | 22 | 57 |
| | | AGYE EW | 270 | 1800 | A | 0.02 | 0.40 | 0.32 | 1.75 | 100 | 0 | 38 |
| | | AGYE NS | 270 | 1800 | A | 0.02 | 0.80 | 0.50 | 0.80 | 100 | 0 | 39 |
| **OTHER SELECTED RECORDS** | | | | | | | | | | | | |
| **MICHOACAN EARTHQUAKE, 1985-09-19 **** | **8.0** | SCT1-M N00E | 425 | 81 | E-F | 0.10 | 2.00 | 2.00 | 2.00 | 183 | 40 | 71 |
| | **8.0** | SCT1-M N90E | 425 | 81 | E-F | 0.17 | 2.00 | 2.00 | 2.00 | 183 | 33 | 39 |
| **CHIAPAS EARTHQUAKE, 2017-09-08 **** | **8.2** | SCT2-C N00E | 744 | 81 | E-F | 0.02 | 1.60 | 1.67 | 1.63 | 348 | 0 | 97 |
| | **8.2** | SCT2-C N90E | 744 | 81 | E-F | 0.02 | 1.85 | 1.48 | 1.85 | 348 | 0 | 68 |
| **PUEBLA EARTHQUAKE, 2017-09-19 **** | **7.1** | SCT2-P N00E | 120 | 81 | E-F | 0.09 | 1.90 | 1.75 | 1.95 | 317 | 42 | 63 |
| | **7.1** | SCT2-P N90E | 120 | 81 | E-F | 0.09 | 1.60 | 1.80 | 1.60 | 317 | 40 | 45 |
| **KOBE EARTHQUAKE, 1995-01-17 ***** | **6.9** | TAK 000 | 1.5 | 256 | D | 0.62 | 1.23 | 1.25 | 1.23 | 41 | 32 | 11 |
| | **6.9** | TAK 090 | 1.5 | 256 | D | 0.67 | 1.23 | 0.30 | 1.23 | 41 | 19 | 10 |
| **LOMA PRIETA EARTHQUAKE, 1989-10-17***** | **6.9** | LGPC 000 | 1.5 | 594 | C | 0.97 | 0.60 | 0.70 | 0.63 | 25 | 17 | 10 |
| | **6.9** | LGPC 090 | 1.5 | 594 | C | 0.59 | 0.60 | 0.40 | 0.60 | 25 | 17 | 7.6 |

**Data from: *IGEPN (Ecuador), **Red Acelerográfica UNAM (Mexico), ***PEER Ground Motion Database(California)**

Regarding attenuation laws, Singaucho et al., 2016 [1] processed 22 earthquake acceleration records and compared the maximum acceleration (PGA) with that predicted by the Abrahamson attenuation model (GMPE) for subduction earthquakes, finding a good fit with the recorded data.

The acceleration time histories of 87 recordings from 29 stations was evaluated in [2]. The ground motions were compared to the subduction Ground Motion Prediction Equation (GMPE) BCHydro (Abrahamson et al.). The median values of recorded spectral acceleration for this event in general fall below the medians values from other subduction events in short periods. At longer periods, the median of this event is similar to the median from other subduction earthquakes.

## 2.2 Effects of records characteristics on elastic and inelastic response spectra

Structure response to earthquakes is function of both: dynamic characteristics of the ground motion (PGA, duration, frequency content) and dynamic characteristics of the structure (period T, ductility ratio $R_\mu$, i.e., the maximum displacement divided by the yield displacement, damping ratio $\xi$, and constitutive relations), Bertero, 1977 [4]. This study uses $\xi = 5\%$ unless another value is indicated. Due to space limitations not all characteristics mentioned will be presented here.

The effect of duration on Elastic Response Spectra (ERS) and Inelastic Response Spectra (IRS) is shown using ACHN-EW and TAK-000. Both records show similar spectral acceleration dominant periods, $T_a = 1.3$ and $T_a = 1.25$, respectively, but durations are different: $t_{dTrf} = 30s$ and $t_{dTrf} = 11$s, respectively, Table 1. Fig. 2 (a) displays ERS and IRS for $R_\mu = 1, 4,$ and 6, showing that duration affects ERS spectral form. However, differences in IRS are not significant.

The effect of frequency content is pointed out by comparing ACHN-EW and SCT1M-N00E records, which exhibit different $T_a$ and similar durations: $t_{dBolt} = 40s$ for both records, Table 1. The records were scaled to 0.25g, Fig. 2 (b) displays ERS and IRS for $R_\mu = 1, 4,$ and 6, for both records. ERS and IRS spectral forms are very different due to differences in $T_a$.

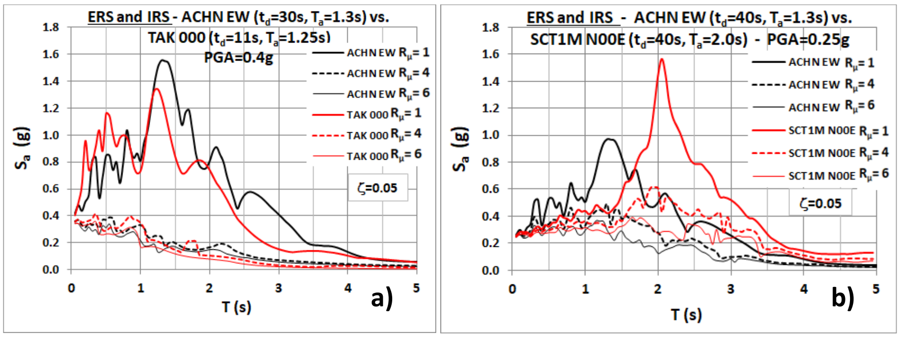


Fig. 2 (a) ERS and IRS for ACHN EW and TAK 000 with same $T_a$ and different $t_d$, varying ductility ratio, both records scaled to 0.4g. Fig. 2 (b) ERS and IRS for ACHN EW and SCT1M N00E same $t_d$ and different $T_a$, varying ductility ratio, both records scaled to 0.25g.

### 2.3 Effects of structure characteristics on elastic and inelastic response spectra

The effects of ductility ratios on structural response is illustrated using Fig. 2 (a) showing that increasing $R_\mu$ reduces significantly the acceleration demands for both records. In contrast, Fig. 2 (b), shows that response reduction due to increasing $R_\mu$ is less important with respect to Fig. 2 (a).

The effect of damping ratio $\xi$ is illustrated in Fig. 3 (a) and Fig. 3 (b) for ERS, using records ACHN-NS and LGPC-000, Table 1. Values for PGA, $T_a$ and durations, are different for the 2 records, and ERS were built for $\xi = 0\%, 2\%, 5\%, 10\%, 20\%$ and $40\%$. The results show that reductions on elastic demands in the long duration ACHN record, are slightly lower than demand reductions in the short duration LGPC record.

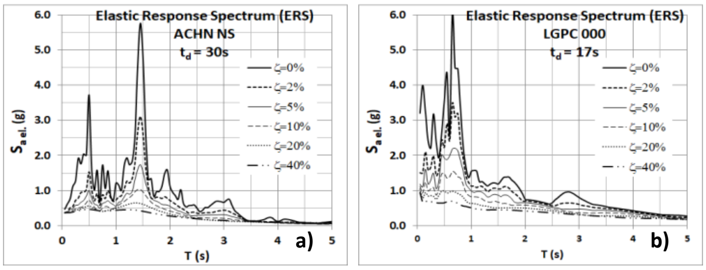


Fig. 3 (a) and 3 (b) Elastic Response Spectra for LGPC 000 and ACHN NS records varying damping ratio

Fig. 4 (a) and Fig. 4 (b) exhibit IRS for $R_\mu = 4$ for ACHN NS and LGPC 000 records and the same values of damping ratio, as above. It is observed that damping induces small acceleration reductions for short periods but, for periods close to T = 1.0s and on, increasing damping increases acceleration demands above



 

$\xi = 2\%$ ordinates.Therefore, designing for $R_\mu = 4$ with a damping ratio larger than 2% will increase acceleration demands for periods larger than 1.00s for these records.

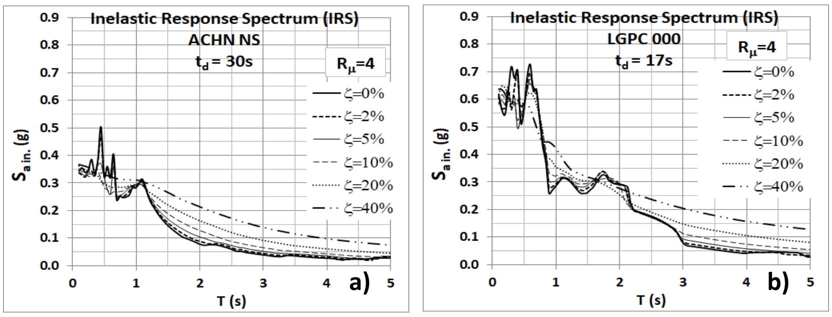


Fig. 4 (a) and 4 (b) Inelastic Response Spectra for LGPC 000 and ACHN NS varying damping ratio,

To explain why demands increase for large damping ratios, Fig. 5 (a) shows, for ACHN, partial history responses of maximum forces and absolute and relative accelerations, velocity and displacement, for a T = 0.74s SDOF, chosen because at that period there is a transition from spectral accelerations reduced by the damping ratio to increased spectral values for increasing values of $\xi$ that vary between $\xi = 5\%$, and $\xi = 40\%$, unit mass, and $R_\mu = 4$ while, Fig. 5 (b) exhibits, the same demands but, for a T = 3s SDOF, for same values of $\xi$, unit mass, and $R_\mu$. Table 2 shows the data for the mentioned parameters for both structures.

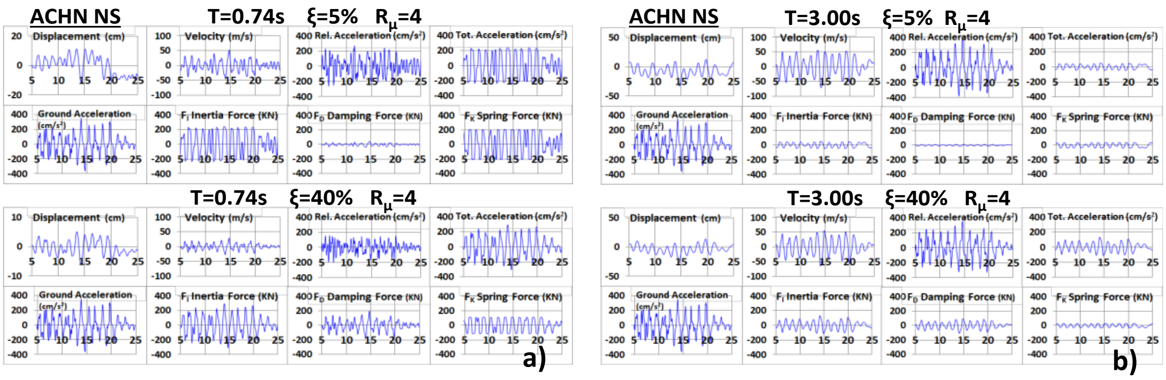


Fig 5 (a) and Fig. 5 (b) Response for ACHN NS record, varying structure period T, but same $R_\mu$ and $\xi$.

Table 2 Forces and responses for increasing damping ratio for two structures.

**ACHN NS** **$R_\mu$=4**

| | T=0.74s | | T=3.0s | |
|---|---|---|---|---|
| | ξ=5% | ξ=40% | ξ=5% | ξ=40% |
| $F_I$ (KN) | -249.3 | -307.9 | 50.6 | 135.2 |
| $F_D$ (KN) | 44.6 | 198.8 | -14.9 | -107.3 |
| $F_K$ (KN) | 204.7 | 109.0 | -35.7 | -28.8 |
| $u_{max}$ (m) | 0.1 | -0.07 | -0.3 | -0.27 |
| $\dot{u}_{max}$ (m/s) | 0.5 | 0.29 | -0.7 | -0.64 |
| $\ddot{u}_{max}$ (g) | 0.27 | -0.20 | 0.40 | 0.35 |
| $(\ddot{u}_g + \ddot{u})_{max}$ (g) | -0.25 | -0.31 | 0.05 | 0.14 |

For each structure, there is force equilibrium Table 2, but forces and responses vary with damping ratio $\xi$ and structure period T.



 

Inertia force and maximum total acceleration increase with increasing $\xi$ for the same T but, both decrease if T augments. Maximum velocity $\dot{u}$ and maximum displacement $u$ reduce if $\xi$ grows for the same T but, rice for increasing T. The same occurs for damping and stiffness forces.

The damping coefficient $c = 4\pi m \frac{\xi}{T}$ increases with increasing $\xi$ for the same T but, decreases for a larger T. Velocity become lees for the same T but, grows up if T also grows. Therefore, $f_d$ increases for the same T but, decreases for the large T because c becomes less for the large T.

The largest force is the total acceleration inertia force $F_I$ which increases for $\xi = 40\%$, respect to $\xi = 5\%$ for both values of T, but, the augment of $F_I$ is larger for the large T so, this is the reason why total acceleration demands increase whit increasing $\xi$ and increasing period T.

In addition, the shorter the record duration and record period $T_a$, as LGPC-000 Fig. 4 (b), the larger the increase of IRS demands over $\xi = 2\%$ demands and the increase starts at about T = 1.0s for both records.

To clarify the elastic demands for large $\xi$, the analysis of elastic forces and responses of ACHN-NS for $\xi = 5\%$ and $\xi = 40\%$, is amplified here and compared to IRS results for $\xi = 40\%$.

Fig. 6 presents ERS for ACHN-NS computed for $\xi = 5\%$ and $\xi = 40\%$ and T = 3s, and Table 3, results of forces and responses.

Fig. 6 shows that for $\xi = 40\%$ and T = 3s, the total acceleration spectrum demand $S_{ael} = 0.15g$ so, the inertia force, for a unit mass is $F_I = 147.9KN$ Table 3. Therefore, increasing damping reduces elastic demands.

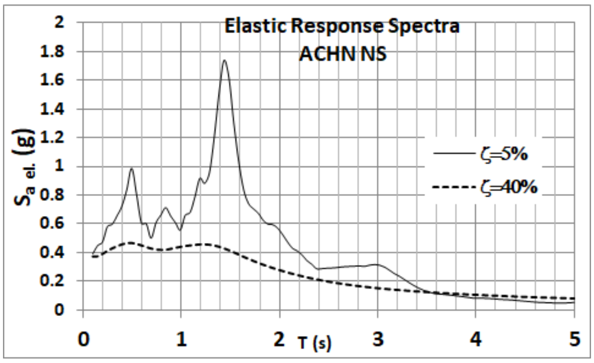


Fig. 6 Elastic Response Spectra for ACHN NS record for 5% and 40% damping ratios

Table 3 Elastic Forces and responses for increasing damping ratio for a structure

| ACHN NS | $R_\mu$=1 (Elastic) | |
|---|---|---|
| | T=3.0s | |
| | ξ=5% | ξ=40% |
| $F_I$ (KN) | 305.9 | 147.9 |
| $F_D$ (KN) | -31.6 | 123.1 |
| $F_K$ (KN) | -304.0 | -95.4 |
| $u_{max}$ (m) | -0.70 | -0.22 |
| $\dot{u}_{max}$ (m/s) | -1.52 | 0.74 |
| $\ddot{u}_{max}$ (g) | 0.47 | 0.40 |
| $(\ddot{u}_g + \ddot{u})_{max}$ (g) | 0.31 | 0.15 |

From Table 2, the inertia force for $\xi = 40\%$, $R_\mu = 4$, and T = 3s, is $F_I = 135.2KN = S_{ain}$ . This inelastic demand is less but, close to the elastic demand, $F_I = 147.9KN$, for the same period and damping ratio. Therefore, large damping on inelastic response amplifies inelastic total acceleration demands which, for $\xi = 40\%$, and for ACHN-NS, are close to elastic demands. This means that for $R_\mu = 4$ and $\xi = 40\%$, design should be close to elastic for the T = 3s structure.

The effect of constitutive relations on IRS is examined using a SDOF system subjected to ACHN-NS and TAK-000, both with similar periods but, different durations and PGA, and to APED-EW and SCT1M-N90E, both with different periods, durations, and PGA. To build IRS, 2 constitutive relations are used: the EPP (Elastic-Perfectly Plastic) and Clough models, for $R_\mu = 4$. Fig. 7 (a) and Fig. 7 (b), show IRS for ACHN and TAK records, and Fig. 7 (c) and Fig. 7 (d) IRS for APED and SCT1M. For Clough model [5], the strain hardening was estimated as 1/30 of the elastic stiffness. Results are shown in Table 3 for T = 0.5s, T = 1.0s, and T = 5s, and $R_\mu = 4$.

Differences on $S_{ain}$ demand are not significant except for the T = 2s SDOF, Fig. 8 (a), Fig. 8 (b) that show hysteretic responses for APED and SCT1M. Consider the variation of SCT1M demands Table 4, and Fig. 8 (b) that presents hysteretic responses of the SDOF for the EPP and Clough models, respectively. If $F$ is the spring force and $W$ is the weight, it is observed that the maximum ratio $\frac{F}{W}$ in SCT1M, changes from 0.15 in the EPP model to 0.10 in Clough model, and the reason is explained in Fig. 8 (b) and Fig. 9.

Let $R_r$, or strength reduction factor, be defined as the maximum force of the elastic system divided by the yield force. It can be seen that up to T = 1.6s, $R_r \leq (R_\mu = 4)$ and $0.18g \leq S_{ain} \leq 0.22g$, Fig. 9. From then on, to keep $R_\mu = 4$, Clough model, $R_r$ starts to grow up reaching 11.5 for T = 2.0s so, the ratio $\frac{F}{W}$ reaches 0.1. EPP model does not degrade and for T = 2s, $R_r = 7.7$ is enough to keep $R_\mu = 4$ and $\frac{F}{W} = 0.15$. Clough model for most period values requires larger $R_r$ values than EPP model to keep the same ductility ratio. Differences in hysteretic responses are larger for APED, Fig. 8 (a) but, the analysis performed is valid for both IRS records.

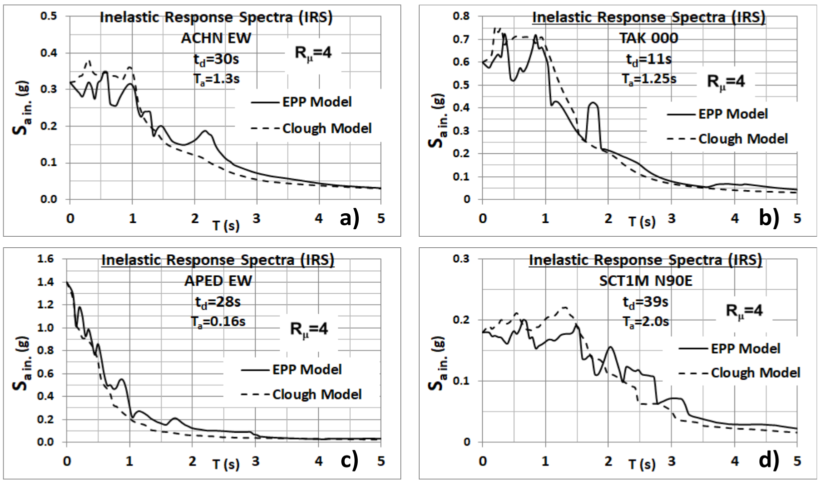


Fig. 7 (a), Fig. 7 (b), Fig. 7 (c) and Fig. 7 (d) Inelastic Response Spectra for ACHN EW, TAK 000, APED EW, SCT1M N90E for two different hysteretic models and $R_\mu$=4



 

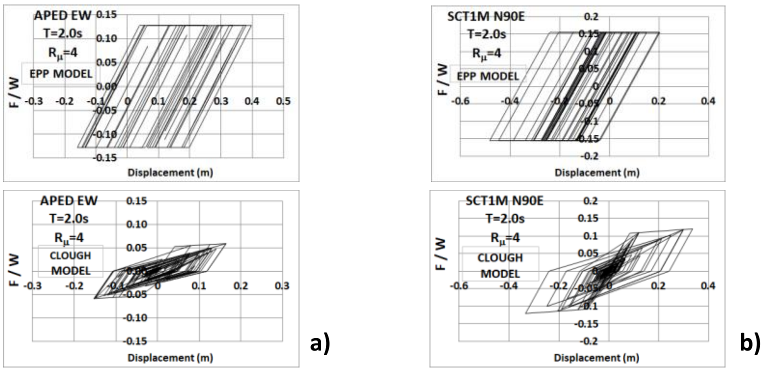


Fig. 8 a) and b) Hysteretic responses for APED EW and SCT1M N90E of a T=2.0s structure for two different hysteretic models and $R_\mu$=4

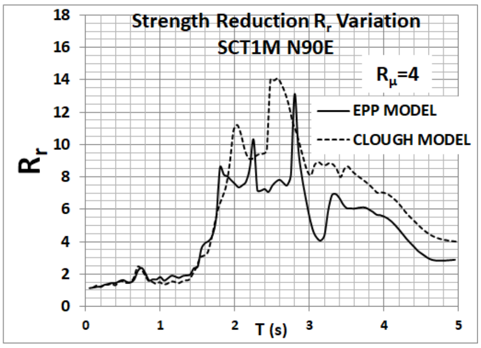


Fig. 9 Variations of strength reduction $R_r$ vs.T for $R_\mu$=4 and two hysteretic models for the SCT1M N90E record.

Table 4 Results of $S_a$ for three structures under 4 records using 2 hysteretic models

| Record | $S_{a\ in.}$ (g) | | | | | |
|---|---|---|---|---|---|---|
| | T=0.5s $R_\mu$=4 | | T=1.0s $R_\mu$=4 | | T=2.0s $R_\mu$=4 | |
| | EPP | Clough | EPP | Clough | EPP | Clough |
| ACHN EW | 0.33 | 0.34 | 0.30 | 0.35 | 0.16 | 0.12 |
| TAK 000 | 0.52 | 0.70 | 0.63 | 0.70 | 0.22 | 0.21 |
| APED EW | 0.85 | 0.70 | 0.33 | 0.22 | 0.13 | 0.06 |
| SCT1M N90E | 0.18 | 0.20 | 0.16 | 0.20 | 0.15 | 0.10 |

For large T, results from EPP model could mislead a design process because it requires to design for a large force demand since there is no stiffness degradation in the hysteretic model. However, from $R_\mu > 1.0$ damage occurs and there will be stiffness deterioration therefore, Clough model results are more realistic. It should mention that there are improved models like Giuffre, Pinto, 1970 [6], Menegotto, Pinto, 1973 [7] which gives even more precise results, Lara, 2011 [8].

### 2.4 Proposed fitting for the descending branch of displacement spectra for soft soils

Regarding spectral displacements, Fig. 10 (a) exhibits ERS for the 6 components captured on soft soil records ACHN-EW, ACHN-NS, AGY1-NS, AGY1-EW, and AGY2-NS, AGY2EW. It is noticed that ERS start displacement reductions at about $T = 1.7s$. therefore, a fitting process was performed for the 6 records. The coordinates to start the fitting are from ACHN-NS, the largest spectral value of the records used. For $\xi = 5\%$: ordinate: displacement = 0.68m, abscissa: period: 1.7s. The proposed exponential curve for fitting is $Y = \frac{A}{X^n}$, and it will be seen that the best fitting is for $n = 1$ so, the equation for the descending branch of the displacement spectra for soft soils records captured in the coastal area of Ecuador during the Pedernales, 2016 earthquake can be represented by:

$$S_d = \frac{1.9x0.68}{T^{1.2}} \text{ (in meters)} \tag{1}$$

The descending branch of the displacement spectra and the fitting curve are shown in Fig. 10 (b). Notice that if $n > 1$, the fitting curve moves downwards.

To improve the fitting SCT soft soil records are included and the result is in Fig. 10 (c). The equation representing the descending branch for spectral displacement is:

$$S_d = \frac{1.7x0.68}{T} \text{ (in meters)} \tag{2}$$

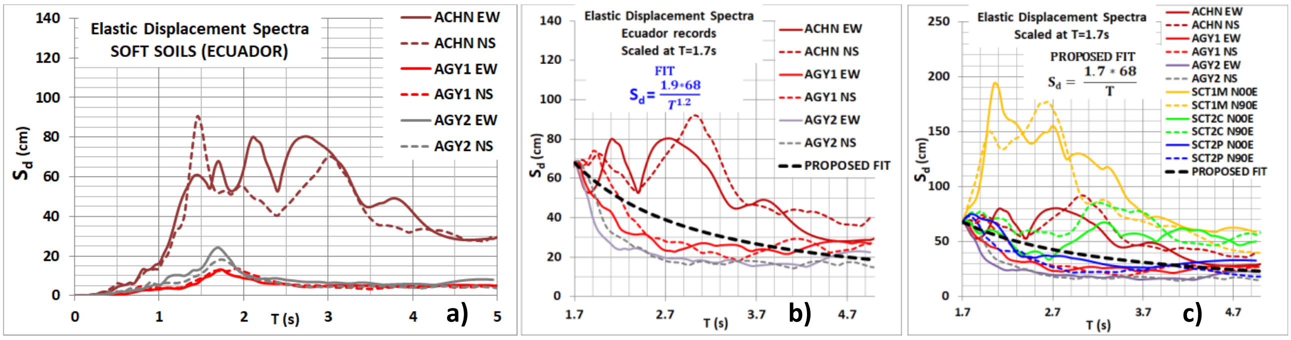


Fig. 10 (a) Elastic Displacement Spectra for 6 components of ACHN, AGY1, AGY2 stations and Fig. 10 (b), fitting curve for the records scaled to T=1.7s and maximum displacement of 0.68m. Fig. 10 (c) fitting curve for the 6 records and 6 records from SCT

## 3. Elastic relative input energy spectra

Fig. 11 shows the elastic input energy spectra for the records used in this study, Table 1. The maximum peak of the energy spectra corresponds to the energy period $T_e$.

ACHN-NS contains the maximum energy of the records used and $T_e = 1.45s$.

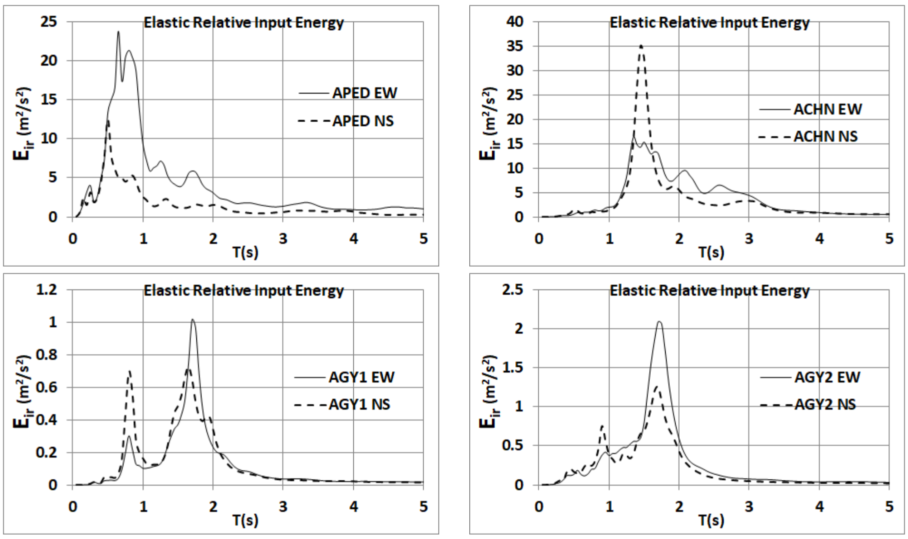


Fig. 11 Elastic input energy spectra for the records used in this study



 

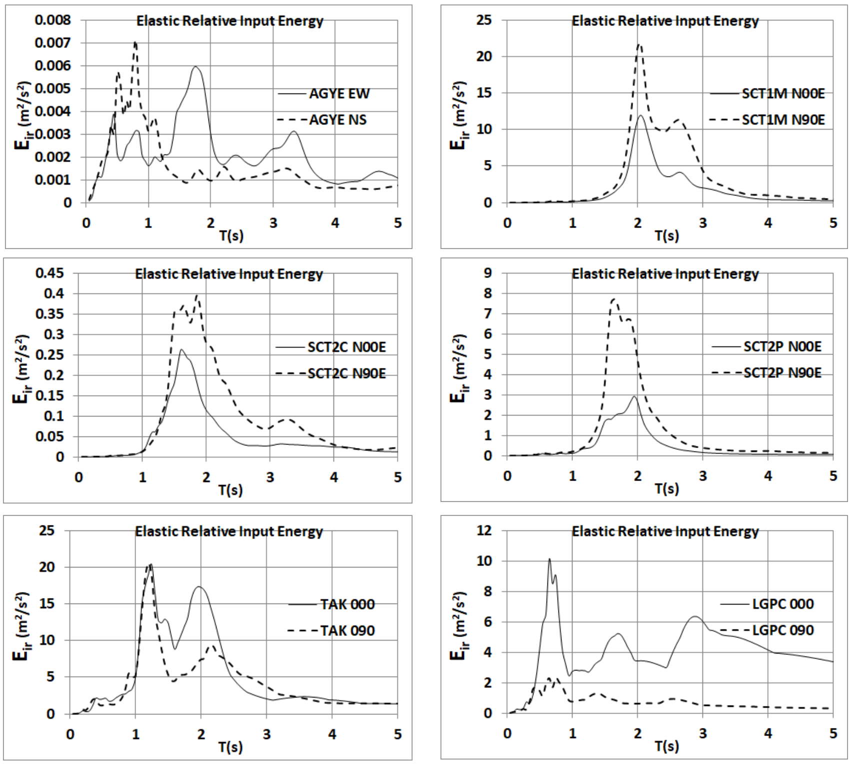


Fig. 11 (cont.) Elastic input energy spectra for the records used in this study

## 4. Conclusions

The predominant periods $T_g$, $T_a$, $T_e$ of the soft soil records for Pedernales earthquake show that the ground motion energy is concentrated in long period values, particularly in the 1.3 s - 1.7s range, but also with some peaks at 0.3 s - 0.5 s. These values are somewhat lower than the predominat period of about 2s of the SCT1-M record observed in the Michoacan earthquake.

The AGY1, AGY2 and AGYE records show a significant soil/rock amplification of PGA, between 3 and 5, similar to the amplification of about 4 observed in the SCT1-M and CUMV records during the Michoacan 1985 Earthquake.

Regarding effects of record duration $t_d$, frequency content, and soil type on ERS and IRS, for same PGA and similar $T_a$ but, different, $t_d$ and soil, IRS ordinates for ACHN-EW and TAK-000 result about similar however, when $t_{d,}$ PGA, and soil type are similar but, $T_a$ is different, IRS ordinates for ACHN keep the same tendency, although there are some variations in amplitudes due to change in PGA but, SCT1M-N00E IRS ordinates vary significantly.

The results show that duration, frequency content, expressed by $T_a$, and soil type have an effect on ACHN IRS. There are no variations on ACHN ERS, as expected.

Effect of damping ratio $\xi$ on ERS for ACHN-NS and LGPC-000 show expected results: the larger the damping ratio, the larger the reduction of spectral amplitudes. However, the effect of $\xi$ on IRS for both records is different. $T_a$, PGA, $t_d$ and soil type are different for both records and $\xi$ reduces amplitudes up to about T = 0.7s. From then on, except for punctual periods, IRS ordinates grow respect to $\xi = 2\%$.. Therefore, if $\xi$ is increased, when design is based on $R_\mu > 1$, IRS demands will increase for T > 0.74s.



 

To study the inelastic response spectra (IRS), APED-EW and SCT1M-N90E records were considered under 2 hysteretic models: EPP and Clough. Both records have different PGA, $T_a$, $t_d$, and are located on different soil type. The result shows that for APED, $R_\mu = 4$ and EPP model, maximum shear force ratio demand is 0.14, while for Clough model the ratio is 0.05. Demands for $\frac{F}{w}$ in SCT1M for the same $R_\mu$ and EPP model is 0.15, but for Clough model reaches 0.1. It was shown that for values of strength reduction, used to build IRS, $R_r < R_\mu$, the SDOF response is inelastic but, amplitude variations in IRS are very low. When $R_r > R_\mu$, amplitudes decrease because, to keep $R_\mu = 4$ fixed, $R_r$ must vary. The stiffness degrading Clough model requires higher values of $R_r$ to comply with $R_\mu$. For short $T_a$, large PGA, $t_d$ about 70% of ACHN, and 40% of SCT1M, and soil type D, like APED, lateral force ratios for EPP are large while, for Clough are very small. Since Clough model degrades, it is a more realistic model to use than EPP model.

Finally, a proposal for the descending branch of the displacement spectra for soft soils is performed for the soft soil coastal records and then an improvement is performed including soft soil records from CD-MEX, captured in SCT station.

## 5. References

[1] Singaucho J.C., Laurendeau A., Viracucha C., Ruiz M., 2016. Observaciones del sismo del 16 de Abril de 2016 de magnitud Mw7.8, Intensidades y Aceleraciones. Instituto Geofisico, Escuela Politecnica Nacional (IGEPN), Quito.

[2] Geotechnical Extreme Events Reconnaissance (GEER) Association. 2016. “GEER-ATC Earthquake Reconnaissance Muisne, Ecuador, Earthquake Report”.

[3] Laurendeau, A. Perrault, M. 2016. (IGEPN-LMI SVAN) “Preliminary Observations of Site Effects During the Mw 7.8 Pedernales (Ecuador) Earthquake of April 16th 2016”. 5th IASPEI / IAEE International Symposium: Effects of Surface Geology on Seismic Motion

[4] Bertero, V.V. 1977. CE-227 “Structural Design for dynamic loads”. UC Berkeley Course.

[5] Clough, R. 1966. “Effect of Stiffness Degradation on Earthquake Ductility Requirements”.

[6] Giuffre, A. and Pinto, P.E. 1970. “Il Comportamento del Cemento Armato per Sollecitazioni Cicliche di Forte Intensità”. Giornale del Genio Civile.

[7] Menegotto, M. and Pinto, P.E. 1973. “Method of Analysis for Cyclically Loaded Reinforced Concrete Plane Frames Including Changes in Geometry and Non-Elastic Behavior of Elements under Combined Normal Force and Bending”.

[8] Lara, O. (2011). “The flexural seismic resistant design of reinforced concrete bridge columns”. Ph.D. Thesis, University of British Columbia, Vancouver, Canada.


 